3

PET/CT

Joshua D. Schaefferkoetter, Eric R. Carlson and Amy K. LeBlanc
University of Tennessee Medical Center
United States

1. Introduction

Clinical imaging exists for the noninvasive, *in vivo* study of disease in the body. Modalities such as computed tomography (CT) and magnetic resonance imaging (MRI) do this by providing information about patient anatomy, so physicians can identify physical abnormalities in the tissue morphology. In contrast, molecular imaging modalities like positron emission tomography (PET) do not describe the anatomy directly, but rather track specific biological processes. This enables the investigation of bodily function, allowing the identification of abnormalities in tissue physiology.

Central to molecular imaging is the molecule, or more specifically, the radiopharmaceutical. PET is used to study many processes including blood flow, tissue perfusion, neurological function, cellular proliferation, and tumor metabolism, and each application uses a unique radiotracer that has been engineered to track a specific molecule or biochemical process. For example, the most common radiopharmaceutical used in PET today is 2-deoxy-2-(^{18}F)fluoro-D-glucose or ^{18}F-FDG. In this tracer, ^{18}F (a radioactive isotope of Fluorine) is substituted in place of the 2' hydroxyl group in the glucose molecule. FDG is chemically similar to glucose, and so it begins to follow the same metabolic pathway. The accumulation of FDG is subsequently used as an index of tissue metabolism. PET forms an image by measuring (estimating) the spatiotemporal distribution of the biomarker.

Information about cellular metabolism proves especially useful in oncology, as rapidly growing tumors have increased energy demands. (Warburg, Posener et al. 1931) In the clinical setting, PET provides physicians with a standardized tool for the assessment, diagnosis, and treatment planning of neoplastic diseases. Many developments have facilitated its integration into the clinic, but few as rapidly as the addition of the CT modality, and now the hybrid PET/CT.

In modern PET/CT, the CT transmission scan is integral to important calculations in the processing of the PET data. Additionally, this configuration provides information about anatomy as well as physiology. The influence of the combined modality provides an unsurpassed level of patient care. Physicians are able to better diagnose disease and plan and monitor response to treatment more effectively.

2. Background

Before exploring the benefit of adding CT to PET, it is worthwhile to review some basic principles of positron emission tomography. As expected, PET scanners measure the energy released as the result of a positron emission. When an unstable isotope randomly decays, it

can do so in a number of ways. In the case of proton-heavy isotopes like Fluorine-18, the process is positive beta (β^+) decay,[1] where a proton is converted into a neutron, emitting a positron and neutrino.

The positron is the anti-matter counterpart of the electron, namely it has the same mass and spin as the electron, but with the opposite charge. When the ejected positron encounters a nearby electron, the pair self-annihilates, and is converted to pure energy according to Einstein's theory of relativity. This energy is released as two 511keV (the rest mass of the electron and positron) photons, propagating in opposite directions, thus conserving momentum.[2]

The fundamental job of the PET tomograph is to detect these annihilation photons and identify pairs arising from the same event. Modern PET scanners consist of multiple rings of detectors and use a detection acceptance timing window of a few nanoseconds, enough time needed for a photon to traverse the full diameter of the transaxial field of view (FOV). When a photon is detected, the timing window is triggered. If another photon is detected within this window, the two are assumed to be from the same annihilation and are registered as a prompt event. The imaginary line connecting the two detectors, along which the event occurred, is termed the line-of-response (LOR) and is recorded for each prompt.

If a second photon is not detected within the timing window, the original detected photon is recorded as a single event and does not have an LOR associated with it. The singles rate is typically a few orders of magnitude greater than the prompts. Additionally, multiple photons can hit the detectors within the timing window, giving rise to multiple events.These are rejected since no LOR can be assigned.

In a routine scan, millions of prompt events are recorded each second, and each LOR has its own prompt count-rate frequency. This frequency is directly related to the total activity contained within a 'tube' connecting the detector faces along the LOR. Thus, PET is a quantitative tool, in that it is possible to measure the activity concentration in a small unit volume in an absolute sense. However, it is important to remember that a PET scanner does not measure the activity distribution directly, but only as linear sums through the distribution, meaning some information is lost. The acquisition data are grouped as sums along parallel LORs, which define angular 'projections', which are then arranged in rows for each successive angle to form sinograms. The estimation of the original object from this projection data is a daunting task that receives ever-increasing attention. (Barrett and Myers 2004)

3. Gantry design

A modern PET scanner consists of a horizontal bed which passes through a circular bore encasing multiple rings of detectors. The port diameter size of a typical gantry is 70-80 cm with an axial field of view (FOV) around 20 cm. The subject is positioned appropriately, and each bed position is scanned for 2-3 minutes.[3]

---

[1] F-18 has a branching fraction of 0.97 which means there is a 3% chance that it will decay via electron capture, (Shapiro 2002) where an innermost orbital electron combines with a nuclear proton to create a nuclear neutron, releasing only a neutrino.

[2] The relative alignment of the initial particle spins and the positron's kinetic energy at the time of annihilation may affect the number and direction of the emitted photons; however, these effects are usually considered negligible in practice. (Valk 2003)

[3] A routine whole-body scan (from the cranial orbits to mid-thigh) typically includes 4-6 bed positions. Melanoma scans of the entire body use as many as twelve.

Today's PET detection systems are scintillation-based; once a 511keV photon strikes a detector crystal, it is converted into light. This light is collected by a system of coupled photomultiplier tubes (PMTs), which then output an electrical pulse. [4] The strength of this pulse determines the initial energy deposited in the crystal and can be used to reject (scatter)events that do not satisfy the energy threshold. The Biograph TruePoint TrueV PET/CT scanner (Siemens Molecular Imaging) employs four rings of 48 detector blocks, each containing an array of 13 x 13 crystals. (Jakoby, Bercier et al.)
The first PET/CT images came from individual systems operated independently from each other. The CT data was manipulated for use in the PET corrections, and the images were registered manually. Modern tomographs contain the PET and CT components within the same gantry, separated by 80 cm axially. (Townsend, Beyer et al. 2003) Software now automates both acquisition processes, as well as data correction, reconstruction, and co-registration of the final images. (Barrett and Myers 2004)

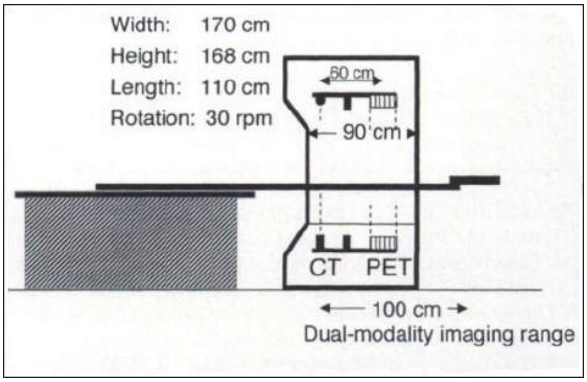

Fig. 1. Schematic diagram of early PET/CT concept. Centers of fields-of-view of PET and CT are 60 cm apart. Combined PET/CT gantry is 110 cm deep, 170 cm high, and 168 cm wide. (Beyer, Townsend et al. 2000)

4. PET Errors

Most reconstruction algorithms treat the data as if they are free of noise or error, but in reality, the PET acquisition process is far from perfect. There are many physical effects that can corrupt the integrity of the data, including photon attenuation, random registration, scattered coincidences, varying detector sensitivity profiles, and gantry geometry. These errors degrade image quality by adding noise to the PET data and must typically be corrected prior to reconstruction for accurate image quantization. It is common in modern PET to perform these data corrections based on large-scale, statistical models of these effects. Every registered prompt event is not the result of a true coincident pair of photons. In fact, each acquired prompt can belong to one of three groups, trues, randoms or scatter. Both randoms and scatter cause the system to associate incorrect LORs to their events and therefore must be corrected.

[4] The PMTs are arranged in a light-sharing configuration (four PMTs per detector block) to reduce cost and packing fraction. (Casey and Nutt 1986)

4.1 Randoms

Random coincidences happen when two photons from different events randomly hit two detectors within the same timing window. These events contain no useful information about the tracer distribution and, because they are random in nature, add smooth background noise to the data. The random coincidence rate is related to the size of the timing window and the singles rates on the detectors.

A few methods have been proposed to model the randoms distribution, including detector singles-based calculations and tail-fitted, Gaussian estimations. (Valk 2003) Currently however, the most commonly implemented technique is the delayed channel method. Here, a timing window is delayed (a few times the timing window length) to acquire a duplicate data stream in parallel to the prompts. The delayed timing window guarantees that any recorded coincident photon pair did *not* belong to the same annihilation event. These delayed data provide accurate representation of the prompt randoms rate and can usuallybe stored independently, allowing post-processing the randoms data to reduce noise.

4.2 Scatter

Scattered events occur when at least one photon of the coincident pair is Compton scattered, deflecting it before hitting the detector ring. Scattering decreases the energy of a photon, so this effect is addressed by acquiring only the photons lying within the photopeak energies. This is accomplished with an appropriate energy-acceptance window (typically 450-650 keV for LSO-based scanners). However, a photon can scatter through a relatively large angle and still have enough energy to be accepted, so many scattered events are not rejected by the energy discriminator. These prompt scatter events are generally treated as a nuisance to the data which should be removed.

In the early years of PET, 2D acquisition was commonly used; disks of lead shielding were positioned between each detector ring to "shadow" the activity arising outside of the direct plane. This decreased the number of randoms and scatter events and simplified the reconstruction process. Now however, 3D, or septaless, acquisition has almost completely replaced its 2D counterpart, due to its increased sensitivity. This change was due to sophisticated correction methods and faster reconstruction algorithms.

Many techniques have been developed to handle scatter correction. Empirical schemes have been used that measure auxiliary data, such as the coincidence rates below 511keV, under the assumption that these lower energy photons must be the result of scattering. By employing multiple energy windows, this auxiliary data is scaled and subtracted from the data in the photopeak window. (Grootoonk, Spinks et al. 1996) Scatter correction based on multiple energy measurements has the advantage of accounting for scatter arising from activity outside of the field of view. However, the auxiliary data are noisy, and their processing requires more computing power. Another technique is to estimate the scatter distribution from prompt counts registered at places known to contain no activity. Scatter has a low frequency, broad distribution with tails that extend beyond the boundaries of the object. These tails can be used to fit a smooth Gaussian function to the scatter distribution. (Stearns 1995) This model performs reasonably well in brain studies but can lead to errors in whole-body scans where the thorax occupies a larger portion of the FOV, resulting in relatively small scatter tails to fit. Some approaches used in 2D PET (with inter-ring septa) are convolution-based integral transformations of the projections. (Bergström, Eriksson et al. 1983) In this method, the scatter

distribution is estimated through the convolution of a spatially dependent scatter "kernel" with the linear projections of the prompt photopeak data. The resulting distribution profiles are then subtracted from the projections to yield scatter-free estimates of the data. It works well in regions of relatively homogeneous density like the brain. This method was developed for 2D PET but has been extended to 3D systems. (Bailey and Meikle 1994)

Modern 3D PET algorithms, however, most commonly use theoretical simulation techniques to correct for scatter. They are arguably the most accurate scatter corrections; in that they attempt to realistically simulate the scattering process. Scatter simulations model the distribution based on the underlying physics of Compton scattering. With an initial estimate of the emitter distribution and a coefficient map of the attenuating material, Klein-Nishina calculations are used to accurately compute the scatter distribution. (Ollinger 1996)

4.3 Attenuation

In addition to the noise in the prompt counts, PET data is also degraded by other effects including attenuation. Compton scattering (in combination with photoelectric absorption) contributes to photon attenuation along each LOR. It is directly related to the amount of matter (tissue) lying in the small tube centered along the LOR, so attenuation is a bigger problem in larger patients.

This loss of count data results in reduced image contrast and detail for internal features, especially those lying deep inside the subject. For a given scan, any volume contains a finite amount of attenuating material, and a coefficient of total linear attenuation can thus be associated to each LOR. These coefficients are ordered and arranged in sinograms, similar to the PET projections, to yield an attenuation coefficient factor (ACF) map. In the simplest sense, attenuation correction is the multiplication of the PET projection data with the ACF map.

Before the introduction of hybrid PET/CT, ACF maps were generated using a 511keV photon transmission scan of the subject prior to the emission measurement. This typically involved rotating a line source of annihilation photons (usually ^{68}Ge) around the patient to provide information about tissue density. Sinogram windowing and data from the subsequent emission measurement were used to remove most of the emission counts from the transmission data. Furthermore, FDG studies have relatively low count rates, and thereis little increase in noise in the correction due to emission activity. (Carson, Daube- Witherspoon et al. 1988) These methods produced accurate ACF maps but required increased patient time in the scanner.

4.4 Normalization

Reconstruction algorithms generally assume the same sensitivity for all LORs, but this is not the case. Differences in crystal elements and photomultiplier tubes, as well as scanner geometry and detector block gaps, all contribute to varying sensitivities for different LORs. As a result, quality control must be performed regularly to assure that the PET scanner is operating optimally and that the sensitivity profiles are known for all LOR projections. This is usually accomplished by scanning a uniform source; since all LORs are illuminated by the same activity concentration, they should yield consistent projections. The (inverse of the) projection data is used to calculate the normalization, i.e. those with higher relative sensitivity appear hotter and will be weighted less in the routine clinical reconstructions.

Noisy data is not the only drawback to emission tomography. With regards to spatial resolution, nuclear imaging modalities are inferior to conventional anatomical imaging. For

example, a typical PET image has an average spatial resolution of 4 mm but that of a typical CT image can be 0.5 mm. This is due to many factors, including the finite size of detector elements, positron range, Compton scatter, and photon non-collinearity.
PET is a complex procedure that is susceptible to many errors. Compared to most other imaging modalities, emission tomography is a relatively noisy process; the amount of available data is fundamentally count-limited by the ethically allowed dose of the radiotracer and convenient patient time inside the scanner. Furthermore, the acquired data are degraded by the many physical distortions previously mentioned. Modern correction techniques are very sophisticated and evolved through innovations in technology and methodology. One of the most significant of these developments was the addition of CT to the PET system.

5. Hybrid PET/CT

The PET/CT scanner, invented by Dr. Ron Nutt and Dr. David Townsend, was originally built at the University of Pittsburgh in 1998. (Townsend, Beyer et al. 1998) CT-based PET corrections had been investigated (Beyer, Kinahan et al. 1994) and the idea to co-register images from different modalities had been proposed for brain studies, (Pelizzari, Chen et al. 1989; Pietrzyk, Herholz et al. 1996) but the hybrid prototype was the first time multiple medical imaging modalities had been combined into a single gantry. This new tool offered improved clinical diagnoses and patient management; it also increased patient comfort and scanner throughput. (Kluetz, Meltzer et al. 2000) The PET/CT scanner was named invention of the year in 2000 by Time Magazine.

5.1 Attenuation

In the past, the data for the PET attenuation correction came from a 10-15 min 511keV transmission scan that was usually administered for each bed position, prior to the emission scan. With the combination of PET and CT, it was possible to generate an ACF map using the CT transmission scan. It is no longer necessary to include PET transmission components with the scanners, eliminating their initial costs as well as those associated with the periodic replacement of decayed sources. The high flux of X-rays leads to lower statistical noise in the ACF measurement and shorter transmission scan leaves longer times for emission scan, further lowering statistical noise for the total scan duration.
The attenuation coefficients are not constant between CT and PET energies. Attenuation is a combination of photon scatter and absorption, and the ratio of these effects is not necessarily the same for different photon energies and material densities. The ACFs found at CT energies, from 40-140 keV, (Shreve and Townsend 2008) require scaling if they are to be used to correct emission data at the 511keV PET energy.
It has been shown that linear scaling methods produce proper ACFs when Compton interactions dominate the attenuation. However they yield poor estimates when photoelectric contributions dominate, as they do at lower CT energies, especially in high- density regions like bone. (Kinahan, Townsend et al. 1998) Thus, accurate attenuation coefficients cannot be rigorously estimated through simple linear scaling. For this reason, density segmentation of different tissue regions has been used successfully, but just aslinear scaling methods have errors caused by the different ratio of attenuation coefficients for bone, segmentation methods produce errors in regions where there are variations in density, such as the lung. (Beyer, Kinahan et al. 1994)

CT-based PET attenuation factors are typically computed through a hybrid combination of both methods. The ratios of attenuation coefficients at CT and PET energies are roughly equal for all tissue except bone (Hubbell and Standards 1969), so current methods segment regions above 300 Hounsfield units as bone tissue and below 300 as soft tissue, respectively. The respective CT-to-PET ACF scaling is 2.26 and 1.90. (Shreve and Townsend 2008) This bi-linear scaling has shown excellent results that perform superior to 511keV transmission methods with lower noise. (Kinahan, Townsend et al. 1998)

5.2 Scatter

Scatter is a major problem in 3D PET (Cherry, Dahlbom et al. 1991); a 511 keV photon traveling in water (or human tissue) has a 50% chance of being scattered by an electron. Consequently, in a clinical scan, 40-60% of the data may be from scattered photon events. Today, the most commonly used correction methods in quantitative clinical 3D PET are based on scatter simulations, which require a coefficient map of the attenuation to realistically model the scattering process. The 511keV ACF scaled from the CT transmission scan is an excellent source of this information.

Monte Carlo simulation is widely used to model scatter and provides the most complete realization of the physical effects associated with it. This technique is used for both evaluation and for the correction itself, but it is currently too slow to be used clinically and islimited to research applications. Instead of accounting for all scattering interactions, the model can be simplified by considering only single scatter events, i.e. events where just one photon of the pair is scattered only once. (Watson, Newport et al. 1996) This simplification isreasonable since it has been shown that 75-80% of scattered coincidences are due to these single scatter events. (Barney, Rogers et al. 1991) It is further justified by the fact that multiple scatter has little effect on the total distribution.

The single scatter simulation (SSS) calculation relies on a volume integral of a scattering kernel over the body, using the relationship between an initial estimate of the activity distribution volume,[5] the reconstructed attenuation volume, and Compton scattering cross- sections calculated from the Klein-Nishina formula. The scatter contribution is calculated forevery LOR across all possible scattering points in the FOV. A faster method has been proposed that is better suited to clinical application. (Watson 2000) With this method, fewer LORs are used in the calculation and continuity is replaced by discrete sampling of the volume data. Thesample points are relative to the transaxial FOV (not the patient) and, since the scatter distribution is relatively smooth, the sampling can be fairly coarse (around 2 cm) without much loss of accuracy. This coarse-scatter sinogram is then interpolated to account for the missing data. Speed is further improved by reusing computed ray sums through the object since scatter calculations in multiple LORs may involve the same photon travel paths.(Mumcuoglu, Leahy et al. 1996) Accuracy is further improved by iterating the scatter calculation, i.e. with each iteration, the previously corrected emission is used in the calculation.

5.3 Reconstruction

In addition to data corrections, the CT information is used in the actual reconstruction process. Modern reconstruction algorithms do not produce images by directly inverting the

[5] different methods have been employed for initial estimates of the emission volume distribution; Watson et al. used 3d reconstructions of the projection data, which include scatter. (Watson, Newport et al. 1996)

projection data, as they did in the past. Instead, they are based on sequential, iterative estimates that converge to an image that best represents the original object. These algorithms are termed expectation maximization (EM) and are well suited to emission tomography because they are less sensitive to noise in the data.

Iterative reconstruction involves the forward and back-projection of simulated data in the attempt to match the measured data as closely as possible. Integral to this method is the system matrix which models the characteristics of the scanning process. It essentially defines the individual probabilities that each projection bin contributes to each image pixel, and vice versa. Ideally, the system matrix accounts for all physical effects of scanner geometry and performance. Attenuation-weighted (AW) algorithms incorporate the attenuation map from the CT scan into the system matrix, and the forward projector is better able to realistically simulate the acquisition process. This increases the accuracy of the physical model unique to the individual scan.

CT data can also be used in the reconstruction scheme as prior information. Prior distributions are sometimes used to regularize the algorithm, enforcing smoothness in the image. Images with high frequency noise (large differences between neighboring pixels) are assigned a lower probability, i.e. they are penalized by the prior. The CT image can be used to segment the image into regions in which uniform tracer concentration is expected. These segmented boundaries are incorporated in a prior so that smoothness is only imposed in regions belonging to the same anatomical region. The use of anatomical images as prior information in *maximum a posteriori* (MAP) reconstructions has yielded improved reconstructions in mathematical phantom simulations. (Gindi, Lee et al. 1991) However thisapproach is typically not used clinically since anatomical information is readily available to be visually interpreted in the fused images.

6. Clinical impact

PET/CT has revolutionized healthcare, and it continues to expand its utility to a wide array of applications. This is illustrated by the growing number of world-wide scanner sales. In 2002, only a couple years after its introduction, PET/CT systems accounted for nearly half of the total PET scanner sales, with the other half belonging to that of dedicated PET scanners. By 2005, PET/CT systems had almost completely overtaken the market. Today, nearly all commercial systems are PET/CT.

The first PET scans were conducted in the 70's at Washington University in St. Louis by Michael Phelps, et al. (Phelps, Hoffman et al. 1975; Phelps, Hoffman et al. 1976) With the development of FDG later that decade, PET gained more attention for its potential clinical value; but due to the difficulties of the imaging process and the high costs of the radiopharmaceuticals, PET was strictly used for research. However, as more PET studies were performed, its clinical utility began to emerge, specifically in the evaluation of disorders of the heart and brain. This led to the first reimbursement of PET in 1995, for myocardial perfusion imaging using Rubidium-82. (Workman and Coleman 2006) The first Medicare reimbursement of FDG-PET scans in oncology came in January of 1998 for the initial staging of non-small-cell lung cancer and the characterization of single pulmonary nodules. (Bietendorf 2004) Coverage for colorectal cancer, lymphoma, melanoma, and many others followed in the next few years.

Fig. 2. Transaxial PET, CT, and fused images taken from a 68-year-old male diagnosed with cholangiocarcinoma. The combined modality provides physiological information as well as anatomical location. The disease is not obvious in the CT image alone, but the PET scan shows an intense focus of metabolic activity medial to the hepatic caudate lobe likely compatible with recurrent malignancy.

Fig. 3. Transaxial PET, CT, and fused images of a 40-year-old female with a history of heavy smoking. The intense metabolic uptake illustrated by the PET scan is accompanied by a 2.2 x 2.8 cm upper lobe mass on the CT image, which was later diagnosed as non-small cell carcinoma.

Today, Medicare provides reimbursement of PET for the diagnoses and monitoring of nearly every form of cancer. Furthermore, PET is also reimbursed for non-cancerous diseases including myocardial perfusion and viability, dementia, neurodegenerative disease, and pre-surgical evaluation of patients with refractory seizures. (Evaluations and Pain).

6.1 Applications in humans

The staging, preoperative assessment and surgical planning of several human cancers realizes theoretical advantages in the use of PET/CT scanning rather than conventional imaging with CT. One such cancer is oral/head and neck cancer. In 2010 the American Cancer Society estimated that 36,540 cases of cancer of the oral cavity and pharynx would be diagnosed among a total of 1,529,560 (2.4%) cancer diagnoses during the same year. (Jemal, Siegel et al. 2010) While most cancers of the oral cavity and pharynx are squamous cell carcinomas, and therefore mucosal in origin and readily detectable on self-examination, the five-year survival rate of such cancers has remained relatively dismal over the past 50 years at 50%. Early detection of the primary cancer and regional lymphatic spread to the cervical lymph nodes might be a means to improving the survival of patients with this disease. To

this end, clinical examination of at risk patients and anatomic imaging with ultrasound (Gor, Langer et al. 2006), computed tomography (Coughlin and Resto 2010), or magnetic resonance imaging (Coughlin and Resto 2010) could possibly represent a means for early detection of cancer of the oral cavity and pharynx, and their regional lymph nodes, thereby leading to more expedient treatment of these cancers with the possibility of a more favorable prognosis. In oncologic terms, a patient with no signs of cervical lymph node involvement is labeled N0, while the patient with palpable cervical lymph node disease is labeled N+. The designation of the neck in the TNM classification (tumor size, neck lymph nodes, metastasis) represents one of the more important aspects of staging of patients with cancer of the oral cavity and pharynx. Specifically, the removal of cervical lymph nodes that identify occult histologic disease has survival benefits to patients, rather than adopting the wait and watch approach to the cervical lymph nodes and resorting to a neck dissection only when clinically palpable lymph nodes are present. Studies have been carried out regarding the imaging criteria that would permit prediction of metastatic disease in the cervical lymph nodes, particularly those that are equivocal in their size and clinical character. Nonetheless, most studies have shown that imaging studies are of limited value for the accurate staging of cervical lymph nodes. (van den Brekel 2000) Owing to the anatomic and physiologic assessment inherent in PET/CT scanning, investigators have looked towards this modality of imaging to determine if increased sensitivity and specificity can be realized when applying this technology to the assessment of the cervical lymph nodes in patients with oral cavity cancers. Such reports have shown that PET/CT is effective for the diagnosis, staging, and restaging of malignancies of the head and neck region. (Myers, Wax et al. 1998; Blodgett, Fukui et al. 2005; Fukui, Blodgett et al. 2005) There was a reported sensitivity of 70-90% and specificity of 80-95% for the patients in whom their cervical lymph nodes are determined to be clinically positive (N+). (Mukherji and Bradford 2006)

In 2007 our molecular imaging research center investigated the role of 18F-FDG PET/CT in the preoperative prediction of the presence and extent of neck disease in patients with oral/head and neck cancer. (Nahmias, Carlson et al. 2007) Seventy patients were enrolled in the study, 47 of whom had a clinically negative neck (N0), 19 of whom had a clinically positive unilateral neck (N+), and 4 of whom had a negative neck on one side and positive on the other. Each patient underwent a PET/CT study prior to undergoing selective neck dissection for N0 disease or modified radical neck dissection for N+ disease. Eighty-three neck dissections were performed in the 70 patients. The neck dissections were oriented as to oncologic levels for the pathologist processing and interpreting the tissues so as to permit correlation between histopathologic findings and the imaging results. One hundred ninety-two (11.4%) of the 1,678 lymph nodes recovered were histologically positive for metastatic disease. The sensitivity and specificity of the PET/CT procedure were 79% and 82% for the N0 neck, and 95% and 25% for the N+ neck. In patients with clinically negative necks, therefore, a negative PET/CT result would not help the oncologic surgeon in the management of the patient due to the rate of false-negative results, but a positive PET/CT result can diagnose metastatic deposits with a high positive predictive value. In patients with clinically positive necks, a positive test will confirm the presence of disease, although false-negative lymph nodes were additionally identified in these clinically positive necks. With respect to the lymph nodes, the sensitivity of the imaging procedure is such that the results could not assist the surgeon in deciding whether the patients with N0 necks benefit by a prophylactic neck

dissection. This realization reinforces the 21st century practice of prophylactic neck dissections in patients with N0 staging associated with cancer of the oral cavity.
In 2009 our molecular imaging research center investigated the use of PET/CT in patients with oral/head and neck cancer with an assessment of the cervical lymph nodes according to time points. In this study, patients underwent a dynamic PET/CT scan consisting of nine time points over 60-115 minutes post-injection. Sixty patients underwent 64 neck dissections whereby 2,170 lymph nodes were evaluated by a static 90-minute study and 118 lymph nodes were studied by time points. A mean SUV (standard uptake value) of hypermetabolic lymph nodes was plotted as a function of time. A lymph node with greater than 10% changewas designated as metastatic. The time point data showed a sensitivity and specificity of58% and 71% respectively.

6.2 Applications in animals

PET/CT is considered novel as a diagnostic technique in clinical veterinary medicine although its use in live animal research endeavors is well recognized. Lack of available equipment and high cost of PET radiopharmaceuticals have limited the use of PET as a clinical diagnostic tool in veterinary medicine, and the few reports available to date have focused on ^{18}FDG PET and PET/CT in veterinary oncology. (Page, Garg et al. 1994; Matwichuk, Daniel et al. 1999; Bassett, Daniel et al. 2002; Bruehlmeier, Kaser Hotz et al.2005; Ballegeer, Forrest et al. 2006; LeBlanc, Jakoby et al. 2009) Currently, the availability of PET for staging and evaluation of response to therapy in clinical veterinary patients is limited to a few locations in the United States. Applications in veterinary oncology will increase as this technology becomes more widely available, aided considerably by regional cyclotron distribution networks for radiopharmaceutical sales.
Both dogs and cats have been used in research settings for novel PET tracer validation studies for many years as their physical size permits serial blood sampling and *in vivo* imaging procedures, in addition to their comparable metabolic and physiologic characteristics. (Larson, Weiden et al. 1981; Larson, Weiden et al. 1981; Page, Garg et al.1994; Cook, Carnes et al. 2007) To date, the majority of radiopharmaceuticals employed for clinical PET in companion animals are commercially available ^{18}F-labelled molecules such as ^{18}FDG and ^{18}FLT. The majority of these studies have been performed in animals with knownor suspected malignancies for the purposes of lesion characterization, tumor staging or for monitoring response to anticancer therapy.
Special considerations for veterinary species undergoing PET/CT imaging center on the necessary use of general anesthesia for patient positioning and immobilization for scanning procedures. PET/CT scans, similar to other cross-sectional imaging techniques such as CT or MRI, are uniformly performed with widely used sedative and anesthetic drugs in veterinary patients. Risks associated with general anesthesia may preclude the use of this diagnostic technique in sick or debilitated animals. There are no standardized recommendations regarding ^{18}FDG dose, but ranges of 0.1 - 0.2 mCi per kg body weight have been reported. (LeBlanc, Jakoby et al. 2008; Lawrence, Vanderhoek et al. 2009; LeBlanc, Jakoby et al. 2009; LeBlanc, Wall et al. 2009) Veterinary patients require 12 hours' fast and use of sedative premedications with cage confinement after ^{18}FDG injection to minimize aberrant uptake of ^{18}FDG in skeletal muscle during the tracer uptake period. Some imaging sites also use general anesthesia for the tracer uptake period for radiation

safety considerations, as it is difficult to control spontaneous urination and/or defecation of radioactive waste in companion animals. Following the tracer uptake period, animals are placed under general anesthesia and the CT and PET data collected as for a human patient scan. (LeBlanc, Jakoby et al. 2008; LeBlanc, Jakoby et al. 2009; LeBlanc, Wall et al. 2009)
Reports of clinical PET and PET/CT in companion animals are sparse in the veterinary literature. Recent studies of whole-body PET and PET/CT in normal dogs and cats demonstrate patterns of ^{18}FDG distribution and SUVs for parenchymal organs to assist in lesion interpretation in disease states. (LeBlanc, Jakoby et al. 2008; LeBlanc, Wall et al. 2009)
A recent investigation of whole-body PET as a staging tool demonstrated the avidity of canine cutaneous mast cell tumor and lymphoma for ^{18}FDG. (LeBlanc, Jakoby et al. 2009) Newer studies have documented ^{18}FDG uptake using PET/CT fusion in specific malignancies, inflammatory brain disease, and have investigated the impact of different anesthesia protocols on physiologic brain uptake of ^{18}FDG. (Lee, Lee et al. ; Lawrence, Vanderhoek et al. 2009; Kang, Kim et al. 2010; Lee, Lee et al. 2010; Lee, Ko et al. 2010)
As studies are published that fully validate its use as a non-invasive whole-body staging method, PET using commercially-available tracers will become a useful and innovative tool in the management of veterinary patients. From a research perspective, companion animals represent robust and relevant models for the validation of new PET tracers in a variety of diseases that affect both humans and animals alike. (Lawrence, Rohren et al.2010)

7. PET/CT: Today and tomorrow

Although a fairly young tool, PET/CT is already irreplaceable in many applications, and the continued improvement of scanner performance promises further clinical integration. However, its full potential remains unrealized largely due to the relative limited availability of useful radiotracers. As new tracers are developed and scanning protocols are further refined, the trend in patient care will become more personalized and tailoredto specific disease, ultimately allowing doctors to provide the best possible care for their patients.

8. References

Bailey, D. and S. Meikle (1994). "A convolution-subtraction scatter correction method for 3D PET." Physics in Medicine and Biology 39: 411.

Ballegeer, E. A., L. J. Forrest, et al. (2006). "PET/CT Following Intensity Modulated Radiation Therapy for Primary Lung Tumor in a Dog." Veterinary Radiology & Ultrasound 47(2): 228-233.

Barney, J., J. Rogers, et al. (1991). "Object shape dependent scatter simulations for PET." Nuclear Science, IEEE Transactions on 38(2): 719-725.

Barrett, H. H. and K. J. Myers (2004). Foundations of image science. Hoboken, NJ, Wiley.

Bassett, C. L. M., G. B. Daniel, et al. (2002). "Characterization of Uptake of 2-Deoxy-2-[18F] Fluoro-D-Glucose by Fungal-Associated Inflammation: The Standardized Uptake Value is Greater for Lesions of Blastomycosis than for Lymphoma in

Dogs with Naturally Occurring Disease." Molecular Imaging & Biology 4(3): 201-207.
Bergström, M., L. Eriksson, et al. (1983). "Correction for scattered radiation in a ring detector positron camera by integral transformation of the projections." Journal of Computer Assisted Tomography 7(1): 42.
Beyer, T., P. Kinahan, et al. (1994). The use of X-ray CT for attenuation correction of PET data, IEEE.
Bietendorf, J. (2004). "FDG PET Reimbursement." Journal of Nuclear Medicine Technology 32(1): 33.
Blodgett, T. M., M. B. Fukui, et al. (2005). "Combined PET-CT in the Head and Neck." Radiographics 25(4): 897.
Bruehlmeier, M., B. Kaser Hotz, et al. (2005). "Measurement of tumor hypoxia in spontaneous canine sarcomas." Veterinary Radiology & Ultrasound 46(4): 348- 354.
Carson, R., M. Daube-Witherspoon, et al. (1988). "A method for postinjection PET transmission measurements with a rotating source." Journal of Nuclear Medicine 29(9): 1558.
Casey, M. and R. Nutt (1986). "A multicrystal two dimensional BGO detector system for positron emission tomography." IEEE Trans. Nucl. Sci 33(1): 460-463.
Cherry, S., M. Dahlbom, et al. (1991). "3D PET using a conventional multislice tomograph without septa." Journal of Computer Assisted Tomography 15(4): 655.
Cook, R. A. H., G. Carnes, et al. (2007). "Respiration-averaged CT for attenuation correction in canine cardiac PET/CT." Journal of Nuclear Medicine 48(5): 811.
Coughlin, A. and V. A. Resto (2010). "Oral Cavity Squamous Cell Carcinoma and the Clinically N0 Neck: The Past, Present, and Future of Sentinel Lymph Node Biopsy." Current oncology reports 12(2): 129-135.
Evaluations, A. P. and P. O. Pain "Medicare National Coverage Determinations Manual."
Fukui, M. B., T. M. Blodgett, et al. (2005). "Combined PET-CT in the Head and Neck." Radiographics 25(4): 913.
Gindi, G., M. Lee, et al. (1991). Bayesian reconstruction of functional images using registered anatomical images as priors, Springer.
Gor, D. M., J. E. Langer, et al. (2006). "Imaging of cervical lymph nodes in head and neck cancer: the basics." Radiologic Clinics of North America 44(1): 101-110.
Grootoonk, S., T. Spinks, et al. (1996). "Correction for scatter in 3D brain PET using a dual energy window method." Physics in Medicine and Biology 41: 2757.
Hubbell, J. and U. S. N. B. o. Standards (1969). Photon cross sections, attenuation coefficients, and energy absorption coefficients from 10 keV to 100 GeV, US National Bureau of Standards; for sale by the Supt. of Docs., US Govt. Print. Off.
Jakoby, B., Y. Bercier, et al. "Performance investigation of a time-of-flight PET/CT scanner."
Jemal, A., R. Siegel, et al. (2010). "Cancer statistics, 2010." CA: A Cancer Journal for Clinicians: caac. 20073v20071.

Kang, B. T., S. G. Kim, et al. (2010). "Correlation between fluorodeoxyglucose positron emission tomography and magnetic resonance imaging findings of non- suppurative meningoencephalitis in 5 dogs." The Canadian Veterinary Journal 51(9): 986.

Kinahan, P., D. Townsend, et al. (1998). "Attenuation correction for a combined 3D PET/CT scanner." Medical Physics 25: 2046.

Kluetz, P., C. Meltzer, et al. (2000). "Combined PET/CT Imaging in Oncology: Impact on Patient Management." Clinical Positron Imaging 3(6): 223-230.

Larson, S. M., P. L. Weiden, et al. (1981). "Positron Imaging Feasibility Studies. II: Characteristics of 2-Deoxyglucose Uptake in Rodent and Canine Neoplasms: Concise Communication." J Nucl Med 22(10): 875-879.

Larson, S. M., P. L. Weiden, et al. (1981). "Positron Imaging Feasibility Studies. I: Characteristics of [3H]Thymidine Uptake in Rodent and Canine Neoplasms: Concise Communication." J Nucl Med 22(10): 869-874.

Lawrence, J., E. Rohren, et al. (2010). "PET/CT today and tomorrow in veterinary cancer diagnosis and monitoring: fundamentals, early results and future perspectives." Veterinary and Comparative Oncology 8(3): 163-187.

Lawrence, J., M. Vanderhoek, et al. (2009). "Use of 3-Deoxy-3-[18F]Fluorothymadine PET/CT for Evaluating Response to Cytotoxic Chemotherapy in Dogs with Non-Hodgkin's Lymphoma." Veterinary Radiology & Ultrasound 50(6): 660- 668.

LeBlanc, A. K., B. Jakoby, et al. (2008). "Thoracic and Abdominal Organ Uptake of 2-Deoxy-2-[18F]Fluoro-D-Glucose (18FDG) with Positron Emission Tomography in the Normal Dog." Veterinary Radiology & Ultrasound 49(2): 182-188.

LeBlanc, A. K., B. W. Jakoby, et al. (2009). "[18F]FDG PET Imaging in Canine Lymphoma and Cutaneous Mast Cell Tumor." Veterinary Radiology & Ultrasound 50(2): 215-223.

LeBlanc, A. K., J. S. Wall, et al. (2009). "Normal Thoracic and Abdominal Distribution of 2-Deoxy-2-[18F]Fluoro-D-Glucose (18FDG) in Adult Cats." Veterinary Radiology & Ultrasound 50(4): 436-441.

Lee, A., M. Lee, et al. (2010). "Imaging Diagnosis-FDG PET/CT of a Canine Splenic Plasma Cell Tumor." Veterinary Radiology & Ultrasound 51(2): 145-147.

Lee, M., J. Ko, et al. (2010). "Effects of Anesthetic Protocol on Normal Canine Brain Uptake of 18F-FDG Assessed by PET/CT." Veterinary Radiology & Ultrasound 51(2): 130-135.

Lee, M., A. Lee, et al. "Characterization of Physiologic 18F-FDG Uptake with PET/CT in Dogs." Veterinary Radiology & Ultrasound.

Matwichuk, C. L., G. B. Daniel, et al. (1999). "Fluorine-18 Fluorodeoxyglucose Accumulation in Blastomyces dermatitidis-Associated Inflammation in a Dog* 1." Clinical Positron Imaging 2(4): 217-221.

Mukherji, S. K. and C. R. Bradford (2006). "Controversies: Is There a Role for Positron-Emission Tomographic CT in the Initial Staging of Head and Neck Squamous Cell Carcinoma?" American Journal of Neuroradiology 27(2): 243.

Mumcuoglu, E., R. Leahy, et al. (1996). "Bayesian reconstruction of PET images: methodology and performance analysis." Physics in Medicine and Biology 41: 1777.

Myers, L. L., M. K. Wax, et al. (1998). "Positron Emission Tomography in the Evaluation of the N0 Neck." The Laryngoscope 108(2): 232-236.

Nahmias, C., E. Carlson, et al. (2007). "Positron Emission Tomography/Computerized Tomography (PET/CT) Scanning for Preoperative Staging of Patients With Oral/Head and Neck Cancer." Journal of Oral and Maxillofacial Surgery 65(12): 2524-2535.

Ollinger, J. (1996). "Model-based scatter correction for fully 3D PET." Physics in Medicine and Biology 41: 153.

Page, R. L., P. K. Garg, et al. (1994). "PET imaging of osteosarcoma in dogs using a fluorine-18-labeled monoclonal antibody Fab fragment." Journal of Nuclear Medicine 35(9): 1506.

Pelizzari, C., G. Chen, et al. (1989). "Accurate three-dimensional registration of CT, PET, and/or MR images of the brain." Journal of Computer Assisted Tomography 13(1): 20.

Phelps, M., E. Hoffman, et al. (1976). "Tomographic images of blood pool and perfusion in brain and heart." Journal of Nuclear Medicine 17(7): 603.

Phelps, M., E. Hoffman, et al. (1975). "Application of annihilation coincidence detection to transaxial reconstruction tomography." Journal of Nuclear Medicine 16(3): 210.

Pietrzyk, U., K. Herholz, et al. (1996). "Clinical applications of registration and fusion of multimodality brain images from PET, SPECT, CT, and MRI*." European journal of radiology 21(3): 174-182.

Shapiro, J. (2002). Radiation protection : a guide for scientists, regulators, and physicians. Cambridge, Mass. [u.a.], Harvard University Press.

Shreve, P. and D. W. Townsend (2008). Clinical PET-CT. New York; London, Springer.

Stearns, C. (1995). "Scatter correction method for 3D PET using 2D fitted Gaussian functions." J Nucl Med 36: 105.

Townsend, D., T. Beyer, et al. (2003). PET/CT scanners: a hardware approach to image fusion, Elsevier.

Townsend, D., T. Beyer, et al. (1998). The SMART scanner: a combined PET/CT tomograph for clinical oncology, IEEE.

Valk, P. E. (2003). Positron emission tomography : basic science and clinical practice. London; New York, Springer.

van den Brekel, M. W. M. (2000). "Lymph node metastases: CT and MRI." European journal of radiology 33(3): 230-238.

Warburg, O., K. Posener, et al. (1931). "The metabolism of the carcinoma cell." The Mechanism of Tumors: 129–169.

Watson, C. (2000). "New, faster, image-based scatter correction for 3D PET." Nuclear Science, IEEE Transactions on 47(4): 1587-1594.

Watson, C., D. Newport, et al. (1996). "A single scatter simulation technique for scatter correction in 3D PET." Three-Dimensional Image Reconstruction in Radiology and Nuclear Medicine 4: 255–268.
Workman, R. and R. Coleman (2006). PET/CT essentials for clinical practice, Springer.